

Crystal Structure Prediction and Isostructurality of Three Small Molecules

Aldi Asmadi, John Kendrick, and Frank J. J. Leusen*^[a]

Abstract: A crystal structure prediction (CSP) study of three small, rigid and structurally related organic compounds (differing only in the position and number of methyl groups) is presented. A tailor-made force field (TMFF; a non-transferable force field specific for each molecule) was constructed with the aid of a dispersion-corrected density functional theory method (the hybrid method). Parameters for all energy terms in each TMFF were fitted to reference data generated by the hybrid method. Each force field was then employed during structure generation. The experimentally observed crystal structures of two of the three molecules were found as the most stable crystal packings in the lists of their force-field-optimised structures. A number of the most stable crystal struc-

tures were re-optimised with the hybrid method. One experimental crystal structure was still calculated to be the most stable structure, whereas for another compound the experimental structure became the third most stable structure according to the hybrid method. For the third molecule, the experimentally observed polymorph, which was found to be the fourth most stable form using its TMFF, became the second most stable form. Good geometrical agreements were observed between the experimental structures and those calculated by both methods.

Keywords: crystal engineering • density functional calculations • lattice energy landscapes • molecular mechanics • polymorphism

The average structural deviation achieved by the TMFFs was almost twice that obtained with the hybrid method. The TMFF approach was extended by exploring the accuracy of a more general TMFF (GTMFF), which involved fitting the force-field parameters to the reference data for all three molecules simultaneously. This GTMFF was slightly less accurate than the individual TMFFs but still of sufficient accuracy to be used in CSP. A study of the isostructural relationships between these molecules and their crystal lattices revealed a potential polymorph of one of the compounds that has not been observed experimentally and that may be accessible in a thorough polymorph screen, through seeding, or through the use of a suitable tailor-made additive.

Introduction

Detailed understanding of polymorphism is of crucial importance for many applications in a range of industries, hence the continued interest in the ability to predict the crystal structures of small organic molecules.^[1–4] Assuming that observed polymorphs correspond to crystal structures with the lowest possible lattice energy, reliable crystal structure prediction (CSP) requires a lattice-energy calculation tool with a high degree of accuracy.^[5–8] Furthermore, the subtle balance between inter- and intra-molecular interactions needs

to be simulated accurately.^[9] Because of the large number of crystal packing alternatives available for a molecule in a small energy window,^[10–13] small changes in molecular structure can lead to very different stable crystal structures.^[14–16] Significant progress in CSP has recently been achieved^[8,17] by calculating the lattice energy with a density functional theory (DFT) approach by means of the VASP package,^[18–21] supplemented by a molecular mechanics correction for the dispersive interactions (the hybrid DFT method).^[13] Applied retrospectively to the first three blind tests in CSP,^[5–7] the hybrid DFT method was used to re-rank all submitted and experimental crystal structures according to the lattice energy.^[22] For eight out of ten molecules, the hybrid method located the observed crystal structures as the most stable form of packing. For the remaining two molecules the hybrid method found the structures corresponding to the experimental structures as the second and the fourth most stable packing alternatives. Two polymorphs are known to exist for three of the ten compounds, and the lattice-energy

[a] Dr. A. Asmadi, Dr. J. Kendrick, Dr. F. J. J. Leusen
Institute of Pharmaceutical Innovation, University of Bradford
Richmond Road, Bradford, BD7 1DP (UK)
Fax: (+44) 1274-236155
E-mail: f.j.j.leusen@bradford.ac.uk

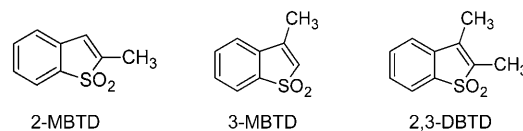
Supporting information for this article is available on the WWW under <http://dx.doi.org/10.1002/chem.200903227>.

calculations correctly ranked these structures as the most stable and the second most stable polymorphs in each of these three cases. In addition, a new polymorph was predicted to exist under pressure for one of the molecules.^[22] The application of the hybrid method in CSP recorded a major success in the 2007 Cambridge Crystallographic Data Centre's blind test by correctly predicting the experimental structures of all four test compounds as the most stable crystal forms.^[8,17] These results demonstrate that the hybrid method is capable of calculating the hypothetical crystal structures corresponding to the observable polymorphs as being among the structures with the most stable lattice energies in the lists of low-energy crystal packings. Together with the hybrid method, an unconventional strategy was introduced that involves the investment of considerable amounts of computational resources and time to generate non-transferable force fields for the CSP target compounds.^[23]

During the search for low-lying minima on the lattice-energy hypersurface, some CSP methods^[24–31] rely on transferable force fields to calculate the lattice energies of sampled crystal structures. These force fields include AMBER,^[32,33] COMPASS,^[34,35] CFF93,^[36,37] CHARMM,^[38,39] Dreiding^[40] and OPLS^[41,42]—each of these has been derived and parameterised to handle a specific class of molecules. Because of their general nature, the energetic and geometric results are usually less than optimal for a specific molecule. Therefore, it is advisable in CSP to refine the transferable force-field results with a quantum mechanical approach.^[13,43,44] The number of crystal structures to be considered in this additional optimisation step depends on the accuracy of the force field used during the search. The more universal the force field, the less accurate the results will be and this leads to an increase in the number of candidate structures that have to be considered in the refinement step. As crystal structure optimisation with quantum mechanics is very computationally intensive, it is important to keep the number of structures selected for the quantum-mechanical refinement to a minimum. If too many structures are selected, the refinement may even become prohibitively time consuming. To address this issue, a logical solution is to build a non-transferable force field specialised for each target molecule^[45] (a tailor-made force field or TMFF).^[23] In essence, a TMFF is developed and parameterised to mimic the molecular structure and the hybrid lattice energy of a particular organic compound in the crystalline environment as accurately as possible with the aid of the hybrid method. The hybrid method calculates the necessary reference data that characterise all possible non-bonded and bonded interactions that could feasibly occur in the crystal lattice. These sets of reference data serve as training sets during the force field fitting.^[23] Considering the studies conducted so far, the application of the TMFF principle in CSP is very promising.

To further test the ability of the hybrid method to predict the most stable crystal packing alternatives on the basis of the lattice energy, three small, rigid and structurally related molecules have been selected for a full CSP study with the TMFF approach. These molecules are derivatives of benzo-

thiophene: 2-methylbenzo[*b*]thiophene 1,1-dioxide (2-MBTD), 3-methylbenzo[*b*]thiophene 1,1-dioxide (3-MBTD) and 2,3-dimethylbenzo[*b*]thiophene 1,1-dioxide (2,3-DBTD). The molecular structures of these three molecules only differ in the position and the number of methyl substituents.



Experimentally, these molecules crystallise in different space groups ($P2_1/c$ for 2-MBTD, $P2_12_12_1$ for 3-MBTD and $P\bar{1}$ for 2,3-DBTD) and adopt distinct packing motifs.^[15,16] Figure 1 shows the packing patterns present in each of the three experimental crystal structures. Viewed along the *b* axis of the unit cell, molecules in the experimental structure of 2-MBTD are stacked parallel and co-planar to one another as illustrated in Figure 1a. Similarly, a parallel stacking is also observed for 2,3-DBTD, however, the molecules are not co-planar in the *c* direction (Figure 1c). In 3-MBTD, a herringbone motif is adopted (Figure 1b).

The study presented here will investigate the stability of each observable crystal packing arrangement in the light of other energetically feasible crystal structures arising from CSP. The influence of the methyl substituents on the observed polymorphs will also be evaluated. Since the three molecular structures are similar, the differences in the number and the positions of the methyl groups will provide some insights as to why no isostructurality is discerned among their experimental crystal structures. The term “isostructurality” used here refers to the similarity observed in the spatial packing arrangement of different compounds.^[46]

Results and Discussion

Conformational analysis with the Dreiding^[40] force field and Gasteiger^[47] charges identified two low-energy conformers for 2-MBTD and 3-MBTD, and four for 2,3-DBTD. For 2-MBTD and 3-MBTD, the structural variations between one conformer and another correspond to the rotation of a single methyl group along its bond, and for 2,3-DBTD the structural variations correspond to the rotation of two methyl groups. These conformational changes are not of significance for each isolated molecule in the gas phase. Only the most stable calculated conformer of each molecule was taken into account for generating reference data related to the non-bonded interactions: electrostatic data, minimisation data, packing data and expansion data. The quantum-mechanical, electrostatic potential in a region outside the van der Waals (vdW) surface of each molecule was calculated using crystal structures with $P1$ symmetry, where the lattice parameters of the crystals had been increased to allow sampling of the potential in this region. The 18 bond increments of 2-MBTD and 3-MBTD and the 19 bond incre-

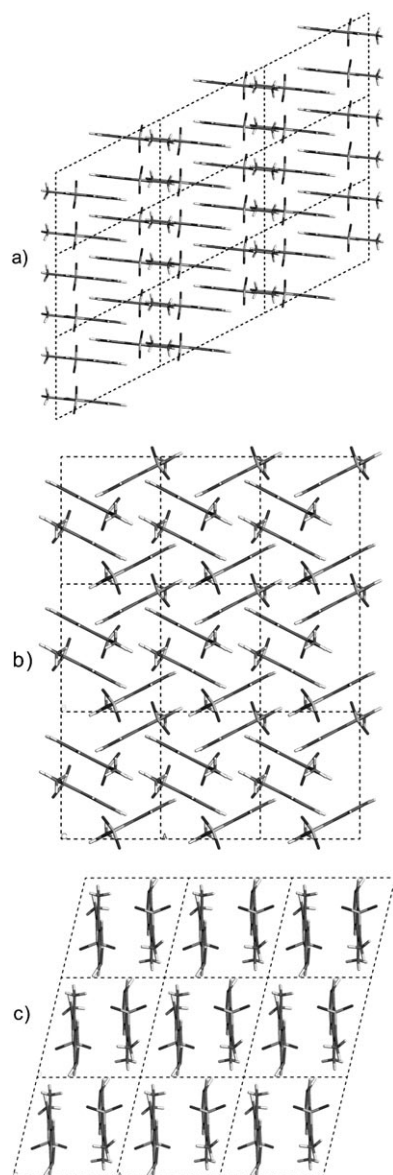


Figure 1. Crystal packing patterns observed in the experimental structures of a) 2-MBTD, b) 3-MBTD and c) 2,3-DBTD.

ments of 2,3-DBTD were optimised to minimise the root mean squared (RMS) deviations (σ_E) between the molecules' quantum-mechanical potentials and the electrostatic potentials calculated from the atomic point charges.

Prior to the calculation of rigid-body minimisation data, a list of rigid-molecule crystal packings in nine space groups was generated for each compound by using its non-bonded force field. In total, 450, 881 and 609 crystal packings were obtained for 2-MBTD, 3-MBTD and 2,3-DBTD, respectively, at pressures of 0 and 5 GPa. Afterwards, 76 structures were selected for 2-MBTD, 58 for 3-MBTD and 61 for 2,3-DBTD to represent all feasible short intermolecular distances in the solid state. The minimised structures at 0 GPa (51 structures for 2-MBTD, 38 for 3-MBTD and 40 for 2,3-DBTD) were further employed to generate the expansion

data. Minimisation data and packing data (at 0 and 5 GPa) and expansion data were used to derive the non-bonded parameters.

The parameters for the bonded interactions were derived by fitting to the conformation data and the wide amplitude data. One conformation data set was calculated for each compound. Wide amplitude data sets were used to characterise the energy barriers associated with any conformational changes due to rotation of the methyl groups. Ten data sets were generated to describe the energy changes related to rotation of the single methyl group in 2-MBTD and 3-MBTD by rotating it from 0 to 60° with an increment of 6°, and 21 data sets to describe the two methyl substituents in 2,3-DBTD. In total, 148 TMFF parameters were fitted for 2-MBTD and 3-MBTD, and 159 parameters for 2,3-DBTD. Additional data on the three TMFFs are available in the Supporting Information.

Hypothetical crystal structures were generated for all compounds with the GRACE software package.^[48] Two hundred structures were obtained for each compound in an energy window of about 0.1 kcal mol⁻¹ per atom above the global-minimum structure. The CSP results for 2-MBTD, 3-MBTD and 2,3-DBTD using their respective TMFFs are summarised in Tables 1–3, respectively. Structures ranked above ten are not listed here.

Initially, the first 20 lowest-energy predictions for each compound were re-optimised with the hybrid method, resulting in a change in ranking of the structures. Calculation of the RMS deviations of the relative energies between the TMFFs and the hybrid method for these 20 structures yielded σ_{ES} of 0.018 kcal mol⁻¹ per atom for 2-MBTD, 0.012 for 3-MBTD and 0.013 for 2,3-DBTD. Based on these figures, additional force-field-optimised structures located in the energy windows of $5\sigma_E$ above the global minima of the force fields were re-optimised with the hybrid method to obtain a very high level of confidence that the most stable crystal structures had been located in the search. In total, and within the $5\sigma_E$ energy range for each of these compounds, 114 low-energy crystal structures were considered for 2-MBTD, 31 structures for 3-MBTD and 75 structures for 2,3-DBTD. Note that the chance of not selecting a stable hypothetical polymorph for optimisation by the hybrid method is the same for each of these three compounds, despite the differences in the number of structures optimised by the hybrid method for each of these molecules. The RMS deviations of the relative energies between the TMFFs and the hybrid method (previously calculated for the first 20 lowest-energy TMFF predictions for each compound) were recalculated by considering all the structures within the $5\sigma_E$ energy windows. The deviations between TMFF and hybrid method remained the same for 2-MBTD (0.018 kcal mol⁻¹ per atom) and 3-MBTD (0.012 kcal mol⁻¹ per atom), but increased from 0.013 to 0.017 kcal mol⁻¹ per atom for 2,3-DBTD. The re-optimisation results for the 10 lowest-energy crystal structures for each molecule are summarised in Tables 1–3. These hybrid-optimised crystal structures are provided in the Supporting Information.

Table 1. The ten lowest-energy crystal structures for 2-MBTD that were predicted according to its TMFF and the hybrid method.

Rank	Entry ^[b]	Tailor made force field			Entry ^[b]	Hybrid method ^[a]		
		$\Delta E^{[c]}$ [kcal mol ⁻¹ per atom]	Density [g cm ⁻³]	Space group		$\Delta E_{\text{Hyb}}^{[d]}$ [kcal mol ⁻¹ per atom]	Density [g cm ⁻³]	Space group
1	2mbtd_00	0.0000	1.467	<i>P2₁/c</i>	2mbtd_00	0.0000	1.440	<i>P2₁/c</i>
2	2mbtd_01	0.0079	1.463	<i>Pbca</i>	2mbtd_01	0.0048	1.431	<i>Pbca</i>
3	2mbtd_02	0.0127	1.442	<i>P2₁/c</i>	2mbtd_03	0.0128	1.443	<i>P2₁/c</i>
4	2mbtd_03	0.0151	1.460	<i>P2₁/c</i>	2mbtd_05	0.0166	1.433	<i>P2₁/c</i>
5	2mbtd_04	0.0167	1.450	<i>Pbcn</i>	2mbtd_02	0.0183	1.420	<i>P2₁/c</i>
6	2mbtd_05	0.0191	1.456	<i>P2₁/c</i>	2mbtd_09	0.0283	1.433	<i>P2₁/c</i>
7	2mbtd_06	0.0357	1.472	<i>P2₁/c</i>	2mbtd_21	0.0322	1.388	<i>P2₁/c</i>
8	2mbtd_07	0.0365	1.440	<i>Pna2₁</i>	2mbtd_14	0.0385	1.397	<i>P2₁</i>
9	2mbtd_08	0.0376	1.429	<i>P2₁/c</i>	2mbtd_28	0.0433	1.420	<i>P2₁/c</i>
10	2mbtd_09	0.0382	1.441	<i>P2₁/c</i>	2mbtd_10	0.0440	1.414	<i>P1</i>

[a] The hybrid-method optimisations were carried out on the final 114 low-energy force field crystal structures covering $5\sigma_E$. [b] Entries written in bold are crystal packings corresponding to the experimental crystal structure. [c] ΔE is the relative energy calculated with the TMFF. [d] ΔE_{Hyb} is the relative energy calculated with the hybrid method.

Table 2. The ten lowest-energy crystal structures for 3-MBTD that were predicted according to its TMFF and the hybrid method.

Rank	Entry ^[b]	Tailor made force field			Entry ^[b]	Hybrid method ^[a]		
		$\Delta E^{[c]}$ [kcal mol ⁻¹ per atom]	Density [g cm ⁻³]	Space group		$\Delta E_{\text{Hyb}}^{[d]}$ [kcal mol ⁻¹ per atom]	Density [g cm ⁻³]	Space group
1	3mbtd_00	0.0000	1.485	<i>P2₁/c</i>	3mbtd_00	0.0000	1.441	<i>P2₁/c</i>
2	3mbtd_01	0.0096	1.481	<i>Pbcn</i>	3mbtd_03	0.0047	1.410	<i>P2₁2₁2₁</i>
3	3mbtd_02	0.0130	1.465	<i>P2₁/c</i>	3mbtd_01	0.0058	1.436	<i>Pbcn</i>
4	3mbtd_03	0.0134	1.433	<i>P2₁2₁2₁</i>	3mbtd_04	0.0080	1.443	<i>P2₁/c</i>
5	3mbtd_04	0.0181	1.463	<i>P2₁/c</i>	3mbtd_14	0.0147	1.425	<i>P2₁/c</i>
6	3mbtd_05	0.0256	1.453	<i>P2₁/c</i>	3mbtd_02	0.0151	1.431	<i>P2₁/c</i>
7	3mbtd_06	0.0318	1.460	<i>C2/c</i>	3mbtd_05	0.0237	1.410	<i>P2₁/c</i>
8	3mbtd_07	0.0350	1.457	<i>P4₃2₁2</i>	3mbtd_22	0.0275	1.406	<i>P2₁/c</i>
9	3mbtd_08	0.0380	1.452	<i>P2₁2₁2₁</i>	3mbtd_12	0.0313	1.419	<i>Pbca</i>
10	3mbtd_09	0.0391	1.458	<i>P2₁/c</i>	3mbtd_21	0.0325	1.420	<i>P2₁/c</i>

[a] The hybrid-method optimisations were carried out on the final 31 low-energy force field crystal structures covering $5\sigma_E$. [b] Entries written in bold are crystal packings corresponding to the experimental crystal structure. [c] ΔE is the relative energy calculated with the TMFF. [d] ΔE_{Hyb} is the relative energy calculated with the hybrid method.

Table 3. The ten lowest-energy crystal structures for 2,3-DBTD that were predicted according to its TMFF and the hybrid method.

Rank	Entry ^[b]	Tailor made force field			Entry ^[b]	Hybrid method ^[a]		
		$\Delta E^{[c]}$ [kcal mol ⁻¹ per atom]	Density [g cm ⁻³]	Space group		$\Delta E_{\text{Hyb}}^{[d]}$ [kcal mol ⁻¹ per atom]	Density [g cm ⁻³]	Space group
1	23dbtd_00	0.0000	1.394	<i>P1</i>	23dbtd_31	0.0000	1.385	<i>Pbca</i>
2	23dbtd_01	0.0027	1.406	<i>P2₁/c</i>	23dbtd_30	0.0004	1.378	<i>P2₁/c</i>
3	23dbtd_02	0.0039	1.394	<i>P2₁/c</i>	23dbtd_00	0.0012	1.393	<i>P1</i>
4	23dbtd_03	0.0044	1.416	<i>Pbca</i>	23dbtd_02	0.0073	1.382	<i>P2₁/c</i>
5	23dbtd_04	0.0086	1.396	<i>P2₁/c</i>	23dbtd_06	0.0079	1.390	<i>P2₁/c</i>
6	23dbtd_05	0.0099	1.379	<i>P2₁/c</i>	23dbtd_07	0.0126	1.381	<i>P2₁2₁2₁</i>
7	23dbtd_06	0.0107	1.394	<i>P2₁/c</i>	23dbtd_05	0.0126	1.373	<i>P2₁/c</i>
8	23dbtd_07	0.0114	1.383	<i>P2₁2₁2₁</i>	23dbtd_01	0.0147	1.387	<i>P2₁/c</i>
9	23dbtd_08	0.0151	1.403	<i>P2₁/c</i>	23dbtd_04	0.0160	1.376	<i>P2₁/c</i>
10	23dbtd_09	0.0156	1.403	<i>Pbca</i>	23dbtd_18	0.0204	1.388	<i>P2₁/c</i>

[a] The hybrid-method optimisations were carried out on the final 75 low-energy force field crystal structures covering $5\sigma_E$. [b] Entries written in bold are crystal packings corresponding to the experimental crystal structure. [c] ΔE is the relative energy calculated with the TMFF. [d] ΔE_{Hyb} is the relative energy calculated with the hybrid method.

The TMFFs of 2-MBTD and 2,3-DBTD predicted the structure corresponding to the experimentally observed polymorphs (2mbtd_00 in Table 1 and 23dbtd_00 in Table 3) as the most stable structure. The packing arrangement of the experimentally determined crystal structure of 3-MBTD was found as the fourth most stable structure (3mbtd_03 in Table 2). An energy difference of 0.0134 kcal mol⁻¹ per atom (or 0.268 kcal mol⁻¹ per molecule of 3-MBTD) was observed between the global minimum and the experimentally observed crystal structure. The hybrid method predicted the structures corresponding to those observed experimentally at ranks 1, 2 and 3 for 2-MBTD, 3-MBTD and 2,3-DBTD, respectively. The result for 2,3-DBTD is surprising as the TMFF predicted the experimental structure at rank 1. Even more remarkable is the fact that the structures ranked 1 and 2 by the hybrid method were originally ranked 32 and 31, respectively, by the TMFF. This considerable reordering is caused by force-field inaccuracies for this particular packing alternative. This finding illustrates that the TMFF is imperfect. The packing patterns in these two structures display some degree of similarity. Overlaying the TMFF crystal structures ranked 32 and 31 with the crystal packing similarity tool in Mercury CSD 2.0^[49,50] to measure the similarity between them shows that 14 out of 16 molecules can be superimposed perfectly with a RMS deviation of 0.023 Å. Their hybrid lattice energies differ by only 0.0004 kcal mol⁻¹ per atom (or 0.009 kcal mol⁻¹ per molecule).

The hybrid method found the experimental crystal structures of 3-MBTD and 2,3-DBTD at 0.0047 kcal mol⁻¹ per atom (or

0.094 kcal mol⁻¹ per molecule) and 0.0012 kcal mol⁻¹ per atom (or 0.028 kcal mol⁻¹ per molecule) above their global minima, respectively. These small energy differences are consistent with earlier findings^[4] and reflect the errors inherent to these calculations, including the neglect of zero-point energies, thermal corrections and contributions to the free energy from entropy, and errors associated with the DFT calculation, the functional and the empirical vdW corrections. It is also possible that the predicted lower-energy structures are potential polymorphs that have not yet been found, although whether these structures exist in reality would need to be investigated by further crystallisation experiments.

Optimisation results for the experimental crystal structures of all compounds (as stored in the Cambridge Structural Database, CSD^[51,52]) with the TMFFs and the hybrid method are summarised in Table 4. The quality of the geometric results is evaluated by calculating the relative difference (Δ) in each lattice parameter, the cell deformation D (as defined previously^[13]) and the RMS deviation in non-hydrogen atomic positions. In general, both methods reproduce the geometries of experimentally determined polymorphs well. The geometric results obtained with the hybrid method agree better with the experimental data than the results obtained with the TMFFs, as indicated by the D values and RMS deviations. The largest discrepancies are found for 2,3-DBTD, which crystallises in the space group $P\bar{1}$ with additional degrees of freedom in comparison to the other two

compounds. Superpositions of the experimental structures with the corresponding TMFF- and hybrid-method-optimised structures are shown in Figure 2. The hybrid-optimised structures are available in the Supporting Information.

In order to explore whether the TMFF concept can be extended to create a highly accurate force field for a specific, small group of similar compounds, a new force field was created (which will be called GTMFF in this discussion) by fitting the force-field parameters to the reference data generated by the hybrid method for all three molecules simultaneously. This GTMFF is transferable between the three molecules. Its accuracy relative to the hybrid method and the three individual TMFFs was evaluated. Considering all structures within a $5\sigma_E$ energy window, for 2-MBTD the accuracy of the TMFF was calculated as 0.018 kcal mol⁻¹ per atom (RMS deviation in relative energy between force-field and hybrid-method results), which increased to 0.022 kcal mol⁻¹ per atom when applying the GTMFF to the same compound. For 3-MBTD the TMFF error of 0.012 kcal mol⁻¹ per atom increased to 0.015 kcal mol⁻¹ per atom when using the GTMFF, and for 2,3-DBTD the error obtained with the TMFF and GTMFF was the same (0.017 kcal mol⁻¹ per atom). The small decreases in accuracy mean that, if this GTMFF were to be used in CSP, in order to achieve the same level of confidence in the predictions in comparison to the use of the individual TMFFs, more force-field-predicted crystal structures would have to be optimised by the hybrid

method, thus requiring more computational effort. Due to time constraints, CSP studies using the GTMFF were not carried out. One has to bear in mind that these three compounds are very similar, which is reflected in the small decreases in accuracy when comparing the TMFFs and the GTMFF. Developing a GTMFF for a group of compounds with larger structural diversity, such as different halogen substituents or amino acids, would probably lead to larger decreases in accuracy in comparison to the use of individual TMFFs.

The GTMFF concept may be of interest in applications where accurate molecular mechanics results are required for a group of similar molecules, for instance the estimation of receptor affinities in rational drug design, but it is of limited practical use in CSP. In order to develop a GTMFF, full sets of reference data have to be gen-

Table 4. Comparison of the experimental crystal structures to the optimised structures obtained with the TMFFs and the hybrid method.

Structure ^[a]	Space group	Density [g cm ⁻³]	Unit cell parameters						D ^[b] [%]	RMS ^[c] [Å]
			a [Å]	b [Å]	c [Å]	α [°]	β [°]	γ [°]		
2-MBTD (CSD ^[d] reference code GAKPEN)										
expl	$P2_1/c$	1.417	10.82	11.47	7.64	90.00	117.14	90.00		
TMFF		1.467	10.60	11.29	7.58	90.00	115.96	90.00	4.30	0.134
Δ [%] ^[e]		3.53	-2.04	-1.60	-0.81	0.00	-1.01	0.00		
hyb		1.440	10.79	11.40	7.56	90.00	116.71	90.00	1.89	0.064
Δ [%] ^[e]		1.64	-0.31	-0.64	-1.13	0.00	-0.37	0.00		
3-MBTD (CSD ^[d] reference code GAKPIR)										
expl	$P2_12_12_1$	1.396	6.92	8.94	13.85	90.00	90.00	90.00		
TMFF		1.433	6.78	8.92	13.81	90.00	90.00	90.00	2.60	0.097
Δ [%] ^[e]		2.65	-2.03	-0.23	-0.31	0.00	0.00	0.00		
hyb		1.410	6.85	8.94	13.95	90.00	90.00	90.00	1.74	0.068
Δ [%] ^[e]		1.02	-0.99	0.01	0.74	0.00	0.00	0.00		
2,3-DBTD (CSD ^[e] reference code GAPMAL)										
expl	$P\bar{1}$	1.356	7.56	8.11	8.60	68.66	86.07	75.95		
TMFF		1.394	7.40	7.96	8.59	68.38	86.84	79.51	6.64	0.233
Δ [%] ^[e]		2.81	-2.00	-1.80	-0.11	-0.41	0.89	4.68		
hyb		1.393	7.48	8.06	8.54	67.70	84.44	76.32	3.69	0.139
Δ [%] ^[e]		2.70	-1.02	-0.52	-0.69	-1.39	-1.90	0.48		

[a] expl = experimental crystal structure; TMFF = force-field-optimised crystal structure; hyb = hybrid-optimised crystal structure. [b] D is calculated as defined in reference [13]. [c] RMS is obtained with the crystal packing similarity tool as implemented in Mercury CSD 2.0^[49,50] with a 16-molecule comparison (ignoring all hydrogen atoms). [d] CSD stands for Cambridge Structural Database.^[51,52] [e] Deviation from experimental value; a positive value of Δ indicates an expansion.

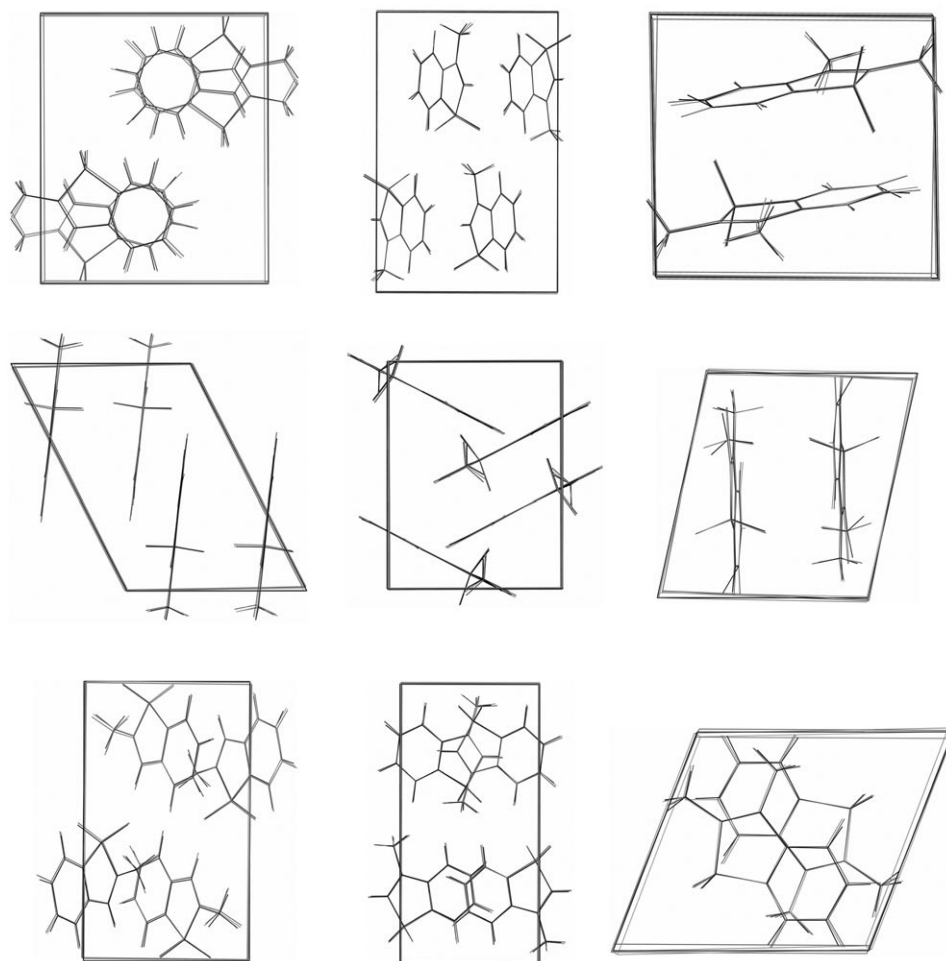


Figure 2. Superposition of the experimentally determined crystal structure (black) with its corresponding TMFF- (dark grey) and hybrid-method-optimised (light grey) crystal structure, shown along the three crystallographic axes for 2-MBTD (left), 3-MBTD (middle) and 2,3-DBTD (right).

erated for each of the molecules studied, which is exactly the same as that required for the development of individual TMFFs. Individual TMFFs are more accurate than a GTMFF, and thus require less computational effort in the final CSP step (re-optimisation of the selected crystal structures by the hybrid method). The additional effort required to develop individual TMFFs in comparison to fitting a GTMFF is less than the additional computational effort required in the final CSP step when using a GTMFF.

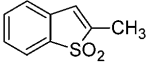
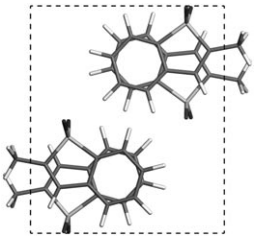
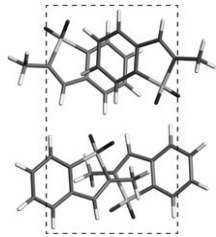
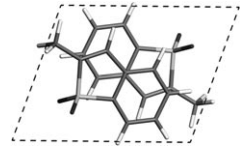
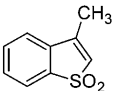
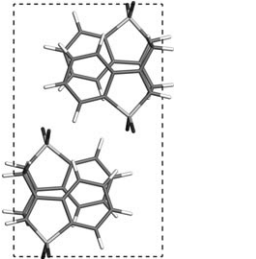
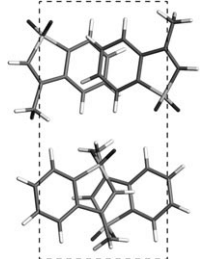
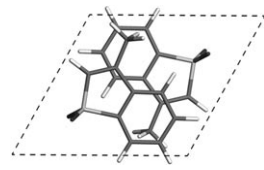
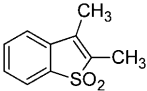
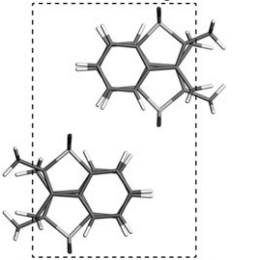
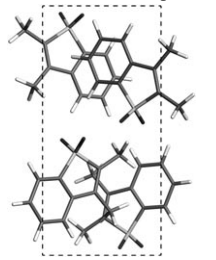
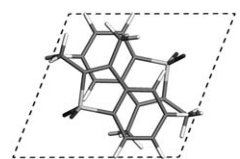
Because the three molecules investigated in this study are similar in molecular structure but significantly different in their crystal structures, it is instructive to construct and study hypothetical crystal structures generated by packing each molecule into the experimentally observed crystal packing patterns of the other two compounds. Table 5 summarises the results of this study. The energetics of the two alternative packing patterns are compared with the native crystal structure for each compound. The stability of each structure, expressed by the hybrid energy, provides some insights as to why isostructurality is not observed among the experimental crystal structures of these molecules.

Most of these crystal structures were located during the CSP searches of the TMFF lattice-energy hypersurfaces, except for the structure containing the 2-MBTD molecule packed into the 3-MBTD crystal. The lattice energy for this structure after minimisation with the hybrid method is $0.1731 \text{ kcal mol}^{-1}$ per atom (or $3.462 \text{ kcal mol}^{-1}$ per molecule) above the global minimum, which is the highest relative energy of all the structures reported in Table 5 and much less stable than any hybrid-optimised structure reported in Table 1. It also explains why this structure was not found in the search for potential crystal structures of 2-MBTD as it is well above the energy cut-off applied. The presence of the methyl group at position 2 disrupts the edge to face interaction between the aromatic units responsible for the stability of the experimentally found polymorph of 3-MBTD, resulting in steric hindrance between the 2-methyl group and the six-member aromatic moiety of the nearest molecule. A similar short contact is also observed in 2,3-DBTD forced into the 3-

MBTD packing, leading to a less stable lattice. In this case, the unfavourable interactions originating from the 2-methyl group are partially offset by favourable interactions involving the 3-methyl substituent.

Note that the 2,3-DBTD molecule packed into the 2-MBTD lattice gives a structure that is slightly more stable than the experimentally observed polymorph of 2,3-DBTD. In fact, this structure corresponds to the second most stable packing alternative found in the CSP of 2,3-DBTD (entry 23dbtd_30 in Table 3). As previously described, its experimental crystal structure is located as the third most stable form by the hybrid method. These results suggest that 2,3-DBTD might be persuaded to crystallise isostructurally to 2-MBTD under the right crystallisation conditions. This may be achieved in a thorough polymorph screen by using a range of solvents and temperatures, by seeding a supersaturated solution of 2,3-DBTD with crystals of 2-MBTD or by the utilisation of a suitable tailor made additive.^[53] Table 6 summarises the differences in the lattice parameters between this hypothetical crystal structure of 2,3-DBTD and the experimental polymorph of 2-MBTD. The introduction

Table 5. The hybrid-optimised crystal structures of the three molecules packed into each other's experimental crystal lattice. Hybrid relative energy is the energy difference between the optimised crystal structure and the global minimum found in CSP.

Molecule	Experimental 2-MBTD	Crystal lattice Experimental 3-MBTD	Experimental 2,3-DBTD
 2-MBTD			
hybrid relative energy	0.0000 kcal mol ⁻¹ per atom	0.1731 kcal mol ⁻¹ per atom	0.0440 kcal mol ⁻¹ per atom
 3-MBTD			
hybrid relative energy	0.0388 kcal mol ⁻¹ per atom	0.0047 kcal mol ⁻¹ per atom	0.0626 kcal mol ⁻¹ per atom
 2,3-DBTD			
hybrid relative energy	0.0004 kcal mol ⁻¹ per atom	0.1017 kcal mol ⁻¹ per atom	0.0012 kcal mol ⁻¹ per atom

of the additional methyl group at position 3 on the ring causes a slight rotation of the molecule and a 20% expansion of the unit cell along the *b* axis. The other unit-cell parameters are not greatly affected. The density shows a small reduction on going from the experimental 2-MBTD structure to the hypothetical 2,3-DBTD structure.

Table 6. Comparison of the lattice parameters of the experimentally determined crystal structure of 2-MBTD and the hypothetical crystal structure of 2,3-DBTD packed into the 2-MBTD lattice.

Structure	Density [g cm ⁻³]	Unit cell parameters ^[a]			
		<i>a</i> [Å]	<i>b</i> [Å]	<i>c</i> [Å]	β [°]
exp 2-MBTD ^[b]	1.417	10.82	11.47	7.64	117.14
opt 2-MBTD ^[c]	1.440	10.79	11.40	7.56	116.71
Δ [%] ^[d]	1.64	-0.31	-0.64	-1.13	-0.37
hyp 2,3-DBTD ^[e]	1.393	10.46	13.80	7.59	122.20
Δ [%] ^[d]	-1.69	-3.33	20.31	-0.65	4.32
Δ [%] ^[f]	-3.26	-3.06	21.05	0.40	4.70

[a] Lattice parameters *a* and γ in these structures are 90° because of the constraints imposed by the *P2₁/c* space group. [b] Experimental crystal structure of 2-MBTD. [c] Hybrid-optimised crystal structure of 2-MBTD. [d] Deviation from experimental value; a negative value of Δ indicates a compression. [e] Hybrid-optimised hypothetical crystal structure of 2,3-DBTD packed into the 2-MBTD lattice. [f] Deviation of hyp 2,3-DBTD from opt 2-MBTD.

Conclusion

Crystal structure prediction studies with tailor-made force fields and a hybrid molecular mechanics/density functional theory approach located the experimental crystal structures of the molecules on their lattice-energy hypersurfaces. Both the TMFF approach and the hybrid method gave good geometric agreement with the experimentally determined crystal structures of 2-MBTD, 3-MBTD and 2,3-DBTD, although the deviations obtained with the hybrid method are nearly half those achieved with the force field approach.

The TMFFs of 2-MBTD and 2,3-DBTD found their experimental structures as the most stable forms, whereas the force field for 3-MBTD found the experimental structure as the fourth most stable alternative. Energy minimisation with the hybrid method changed the lattice energy rankings of 3-MBTD and 2,3-DBTD. The optimisation results using the TMFF and the hybrid method are in good agreement for 2-MBTD. For 3-MBTD the lattice energy ranking of the experimental structure improved from the fourth lowest to the second lowest energy structure with an energy difference of 0.094 kcal mol⁻¹ per molecule between the global minimum and the structure that was experimentally observed. For 2,3-DBTD, however, the hybrid method calculated its experi-

mental crystal structure as the third lowest-energy packing at $0.028 \text{ kcal mol}^{-1}$ per molecule above the global minimum. These small energy differences reflect the approximations used in these simulations (neglect of zero-point energies, thermal corrections and entropy), and the errors associated with the DFT calculation, the functional and the empirical vdW corrections. It is also feasible that the predicted structures close to the global minima are potential polymorphs that have yet to be discovered. Until such crystallisation experiments have been carried out, it is impossible to conclude whether these structures are real polymorphs or not.

A general TMFF (GTMFF) was also created by fitting the force field parameters to the reference data obtained with the hybrid method for all three compounds simultaneously. This GTMFF, which is transferable among the three molecules, was found to be only slightly less accurate than the individual TMFFs and, therefore, could have been used in CSP studies of these three compounds at the expense of additional computational effort in comparison to the use of the individual TMFFs. Although of limited use in CSP, the GTMFF concept may prove useful in other applications such as rational drug design.

Although the three compounds investigated in this study have very similar molecular structures, their crystal structures differ significantly. The results suggest that 2,3-DBTD could crystallise isostructurally to 2-MBTD as the calculated stabilities of these two polymorphs (the experimentally observed polymorph of 2,3-DBTD and the hypothetical polymorph of 2,3-DBTD packed like 2-MBTD) differ by less than $0.01 \text{ kcal mol}^{-1}$ per molecule. It may be possible to crystallise this new 2,3-DBTD polymorph in an experimental polymorph screen by using a range of solvents and temperatures, by seeding a supersaturated solution of 2,3-DBTD with 2-MBTD crystals or by the use of an appropriate tailor made additive.

Computational Methods

The computational procedure used in this study consists of three phases. The first phase involves the parameterisation of a TMFF that reproduces reference data created for each molecule with the hybrid method. Once the TMFF for each molecule has been established, CSP proceeds by using lattice energies calculated by the TMFF to generate crystal structures and to select which structures will be studied further. In the final phase, the hybrid method is used to re-rank the structures selected in the second phase.

In the TMFFs the vdW interactions are described by exponential-6 functions and the electrostatic interactions are described by Coulomb terms that decay as the reciprocal of the distance between point charges (defined by the bond increments). Non-bonded interactions between atoms that are separated by one or two bonds are not considered. Non-bonded interactions between atoms that are part of the same molecule and separated by more than two bonds may be scaled. These intramolecular non-bonded scaling factors are fitted as part of the force-field refinement. The bonded interactions in the TMFFs are described by harmonic functions for the bond-stretch and bond-angle terms, and by overall torsion and inversion functions, which are designed to minimise the number of variables needed in the force field.^[23]

The general procedure for parameterising the force fields has been described elsewhere.^[23] A brief summary is given here along with any details which are specific to the molecules being studied. By using the Dreiding^[40] force field with Gasteiger^[47] charges, all low-energy conformations of the molecules were found by considering their torsional flexibilities. Each low-energy conformer was packed into an expanded *P1* crystal structure and optimised with the hybrid method. Electrostatic potentials were calculated for every unique crystal structure and bond increments were fitted to the electrostatic potentials. Initial non-bonded force fields were derived by using these bond increments and vdW parameters taken from the Dreiding force field.

To probe the non-bonded interactions, sets of rigid-molecule crystal packings based on molecular geometries of the conformers calculated by the hybrid method in the expanded crystals were generated and optimised with the non-bonded force fields at pressures of 0 and 5 GPa. The rigid molecules were packed with one independent molecule in the asymmetric unit into the space groups *P1*, $P\bar{1}$, *P2*, *P2*₁, *Pm*, *Pc*, *C2*, *Cm* and *Cc*. A number of crystal structures were selected at both pressures to represent all feasible non-bonded interactions that may occur in the solid state. These rigid-molecule crystal structures were then optimised with the hybrid method to produce rigid-body minimisation data. The optimised structures at 0 GPa were also used to calculate expansion data.

For each molecule, the non-bonded parameters of the TMFF were determined by fitting to the three sets of data: electrostatic, rigid-body minimisation and expansion data. VdW parameters were refined against rigid-body minimisation and expansion data, whilst keeping the initially obtained bond increments fixed. The vdW parameters and the bond increments were varied simultaneously during the final stage of the non-bonded parameterisation. The resulting non-bonded force fields are suitable for treating the intermolecular interactions of the molecules in their crystalline environments.

Fitting of the bonded parameters required two additional data sets: conformation and wide-amplitude data. Conformational data sets, which probe the variation in energy with bond-length, bond-angle and torsion-angle variations, were calculated using the hybrid method for all unique conformers and wide-amplitude data sets were generated for every flexible bond present in the molecules. With these data sets, the bonded parameters of the TMFFs were determined to describe the intramolecular interactions of the molecules. The final force fields can describe non-bonded and bonded interactions.

A list of crystal packing alternatives was produced for each compound using the structure generation engine implemented in GRACE 1.0^[48] by considering all 230 space groups with a single independent molecule in the asymmetric unit. The structure generation engine sampled hypothetical crystal structures by using a random search that considers the conformational flexibility of each compound as part of the structure generation. All lattice energies were calculated and minimised using each molecule's TMFF. The searches finished when low-energy crystal structures in a pre-defined energy window had been discovered at least twice and had reached the maximum number of allowed structures (200 structures).

The low-energy structures of each compound were further optimised using the hybrid method to provide a final lattice-energy ranking of each structure. To assess the performance of the TMFFs in lattice-energy ranking of the predicted structures, each force field's accuracy was evaluated by comparing lattice energies in the lists of force-field-generated crystal structures with the hybrid-method-optimised crystal structures. The deviations in energy between the lists of the hybrid-optimised structures and the force-field-optimised structures were calculated as root mean squared (RMS) deviations (σ_E) of the energy (in kcal mol^{-1} per atom). Only structures that remained in the same local minimum during optimisation by the force field and the hybrid methods were considered in the calculation of σ_E . The RMS deviation was used to estimate how many structures needed to be optimised by the hybrid method for each compound to be confident that the global-minimum energy structure had been considered.

Acknowledgements

The authors thank Dr. M. A. Neumann for helpful discussions, Avant-garde Materials Simulation for providing a courtesy license to the GRACE software package and the School of Life Sciences at the University of Bradford for funding this project.

- [1] J. A. Kaduk, J. T. Golab, F. J. J. Leusen, *Mater. Res. Bull.* **1998**, *33*, 277–290.
- [2] J. Bauer, J. Morley, S. Spanton, F. J. J. Leusen, R. Henry, S. Hollis, W. Heitmann, A. Mannino, J. Quick, W. Dziki, *J. Pharm. Sci.* **2006**, *95*, 917–928.
- [3] E. F. Paulus, F. J. J. Leusen, M. U. Schmidt, *CrystEngComm* **2007**, *9*, 131–143.
- [4] J. Kendrick, M. D. Gourlay, M. A. Neumann, F. J. J. Leusen, *CrystEngComm* **2009**, *11*, 2391–2399.
- [5] J. P. M. Lommerse, W. D. S. Motherwell, H. L. Ammon, J. D. Dunitz, A. Gavezzotti, D. W. M. Hofmann, F. J. J. Leusen, W. T. M. Mooij, S. L. Price, B. Schweizer, M. U. Schmidt, B. P. van Eijck, P. Verwer, D. E. Williams, *Acta Crystallogr. Sect. A* **2000**, *56*, 697–714.
- [6] W. D. S. Motherwell, H. L. Ammon, J. D. Dunitz, A. Dzyabchenko, P. Erk, A. Gavezzotti, D. W. M. Hofmann, F. J. J. Leusen, J. P. M. Lommerse, W. T. M. Mooij, S. L. Price, H. Scheraga, B. Schweizer, M. U. Schmidt, B. P. van Eijck, P. Verwer, D. E. Williams, *Acta Crystallogr. Sect. A* **2002**, *58*, 647–661.
- [7] G. M. Day, W. D. S. Motherwell, H. L. Ammon, S. X. M. Boerrigter, R. G. Della Valle, E. Venuti, A. Dzyabchenko, J. D. Dunitz, B. Schweizer, B. P. van Eijck, P. Erk, J. C. Facelli, V. E. Bazterra, M. B. Ferraro, D. W. M. Hofmann, F. J. J. Leusen, C. Liang, C. C. Pantelides, P. G. Karamertzanis, S. L. Price, T. C. Lewis, H. Nowell, A. Torrisi, H. A. Scheraga, Y. A. Arnautova, M. U. Schmidt, P. Verwer, *Acta Crystallogr. Sect. A* **2005**, *61*, 511–527.
- [8] G. M. Day, T. G. Cooper, A. J. Cruz-Cabeza, K. E. Hejczyk, H. L. Ammon, S. X. M. Boerrigter, J. S. Tan, R. G. Della Valle, E. Venuti, J. Jose, S. R. Gadre, G. R. Desiraju, T. S. Thakur, B. P. van Eijck, J. C. Facelli, V. E. Bazterra, M. B. Ferraro, D. W. M. Hofmann, M. A. Neumann, F. J. J. Leusen, J. Kendrick, S. L. Price, A. J. Misquitta, P. G. Karamertzanis, G. W. A. Welch, H. A. Scheraga, Y. A. Arnautova, M. U. Schmidt, J. van de Streek, A. K. Wolf, B. Schweizer, *Acta Crystallogr. Sect. A* **2009**, *65*, 107–125.
- [9] P. G. Karamertzanis, G. M. Day, G. W. A. Welch, J. Kendrick, F. J. J. Leusen, M. A. Neumann, S. L. Price, *J. Chem. Phys.* **2008**, *128*, 244708.
- [10] P. Verwer, F. J. J. Leusen, *Rev. Comput. Chem.* **1998**, *12*, 327–365.
- [11] S. L. Price, *Acc. Chem. Res.* **2009**, *42*, 117–126.
- [12] S. L. Price, *Phys. Chem. Chem. Phys.* **2008**, *10*, 1996–2009.
- [13] M. A. Neumann, M.-A. Perrin, *J. Phys. Chem. B* **2005**, *109*, 15531–15541.
- [14] S. A. Barnett, A. Johnston, A. J. Florence, S. L. Price, D. A. Tocher, *Cryst. Growth Des.* **2008**, *8*, 24–36.
- [15] M. S. E. Elfaghi, P. Geneste, J. L. Olive, A. Dubourg, J. Rambaud, J. P. Declercq, *Acta Crystallogr. Sect. C* **1987**, *43*, 2421–2424.
- [16] M. S. E. Elfaghi, P. Geneste, J. L. Olive, J. Rambaud, J. P. Declercq, *Acta Crystallogr. Sect. C* **1988**, *44*, 489–500.
- [17] M. A. Neumann, F. J. J. Leusen, J. Kendrick, *Angew. Chem.* **2008**, *120*, 2461–2464; *Angew. Chem. Int. Ed.* **2008**, *47*, 2427–2430.
- [18] G. Kresse, J. Hafner, *Phys. Rev. B* **1993**, *47*, 558–561.
- [19] G. Kresse, J. Hafner, *Phys. Rev. B* **1994**, *49*, 14251–14269.
- [20] G. Kresse, J. Furthmuller, *Comput. Mater. Sci.* **1996**, *6*, 15–50.
- [21] G. Kresse, J. Furthmuller, *Phys. Rev. B* **1996**, *54*, 11169–11186.
- [22] A. Asmadi, M. A. Neumann, J. Kendrick, P. Girard, M.-A. Perrin, F. J. J. Leusen, *J. Phys. Chem. B* **2009**, *113*, 16303–16313.
- [23] M. A. Neumann, *J. Phys. Chem. B* **2008**, *112*, 9810–9829.
- [24] F. J. J. Leusen, S. Wilke, P. Verwer, G. E. Engel in *Implications of Molecular and Materials Structure for New Technologies, NATO Science Series E, Vol. 360* (Eds.: J. A. K. Howard, F. H. Allen, G. P. Shields), Kluwer Academic Publishers, Dordrecht, **1999**, pp. 303–314.
- [25] A. Gavezzotti, *J. Am. Chem. Soc.* **1991**, *113*, 4622–4629.
- [26] B. P. van Eijck, J. Kroon, *Acta Crystallogr. Sect. A* **2000**, *56*, 535–542.
- [27] J. R. Holden, Z. Y. Du, H. L. Ammon, *J. Comput. Chem.* **1993**, *14*, 422–437.
- [28] M. U. Schmidt, U. Englert, *J. Chem. Soc. Dalton Trans.* **1996**, 2077–2082.
- [29] V. E. Bazterra, M. Thorley, M. B. Ferraro, J. C. Facelli, *J. Chem. Theory Comput.* **2007**, *3*, 201–209.
- [30] D. E. Williams, *Acta Crystallogr. Sect. A* **1996**, *52*, 326–328.
- [31] R. G. Della Valle, E. Venuti, A. Brillante, A. J. Girlando, *Phys. Rev. A* **2008**, *112*, 6715–6722.
- [32] W. D. Cornell, P. Cieplak, C. I. Bayly, I. R. Gould, K. M. Merz, D. M. Ferguson, D. C. Spellmeyer, T. Fox, J. W. Caldwell, P. A. Kollman, *J. Am. Chem. Soc.* **1995**, *117*, 5179–5197.
- [33] S. J. Weiner, P. A. Kollman, D. A. Case, U. C. Singh, C. Ghio, G. Alagona, S. Profeta, P. Weiner, *J. Am. Chem. Soc.* **1984**, *106*, 765–784.
- [34] H. Sun, *J. Phys. Chem. B* **1998**, *102*, 7338–7364.
- [35] H. Sun, P. Ren, J. R. Fried, *Comput. Theor. Polym. Sci.* **1998**, *8*, 229–246.
- [36] J. R. Maple, U. Dinur, A. T. Hagler, *Proc. Natl. Acad. Sci. USA* **1988**, *85*, 5350–5354.
- [37] J. R. Maple, M. J. Hwang, T. P. Stockfish, U. Dinur, M. Waldman, C. S. Ewig, A. T. Hagler, *J. Comput. Chem.* **1994**, *15*, 162–182.
- [38] A. D. MacKerell, D. Bashford, M. Bellott, R. L. Dunbrack, J. D. Evanseck, M. J. Field, S. Fischer, J. Gao, H. Guo, S. Ha, D. Joseph-McCarthy, L. Kuchnir, K. Kuczera, F. T. K. Lau, C. Mattos, S. Michnick, T. Ngo, D. T. Nguyen, B. Prodhom, W. E. Reiher, B. Roux, M. Schlenkrich, J. C. Smith, R. Stote, J. Straub, M. Watanabe, J. Wierkiewicz-Kuczera, D. Yin, M. Karplus, *J. Phys. Chem. B* **1998**, *102*, 3586–3616.
- [39] N. Foloppe, A. D. MacKerell, *J. Comput. Chem.* **2000**, *21*, 86–104.
- [40] S. L. Mayo, B. D. Olafson, W. A. Goddard, *J. Phys. Chem.* **1990**, *94*, 8897–8909.
- [41] W. L. Jorgensen, D. L. Severance, *J. Am. Chem. Soc.* **1990**, *112*, 4768–4774.
- [42] W. L. Jorgensen, D. S. Maxwell, J. TiradoRives, *J. Am. Chem. Soc.* **1996**, *118*, 11225–11236.
- [43] D. J. Willock, S. L. Price, M. Leslie, C. R. A. Catlow, *J. Comput. Chem.* **1995**, *16*, 628–647.
- [44] A. Gavezzotti, *J. Phys. Chem. B* **2003**, *107*, 2344–2353.
- [45] H. R. Karfunkel, F. J. J. Leusen, *Speedup* **1992**, *6*, 43–50.
- [46] L. Fábian, A. Kalman, *Acta Crystallogr. Sect. B* **1999**, *55*, 1099–1108.
- [47] J. Gasteiger, M. Marsili, *Tetrahedron* **1980**, *36*, 3219–3228.
- [48] GRACE (the Generation, Ranking, and Characterization Engine) software package is a product of Avant-garde Materials Simulation SARL, 30 bis, rue du vieil Abreuvoir, F-78100 St-Germain-en-Laye, France, info@avmatsim.eu.
- [49] C. F. Macrae, P. R. Edgington, P. McCabe, E. Pidcock, G. P. Shields, R. Taylor, M. Towler, J. van de Streek, *J. Appl. Crystallogr.* **2006**, *39*, 453–457.
- [50] I. J. Bruno, J. C. Cole, P. R. Edgington, M. Kessler, C. F. Macrae, P. McCabe, J. Pearson, R. Taylor, *Acta Crystallogr. Sect. B* **2002**, *58*, 389–397.
- [51] F. H. Allen, O. Kennard, R. Taylor, *Acc. Chem. Res.* **1983**, *16*, 146–153.
- [52] F. H. Allen, *Acta Crystallogr. Sect. B* **2002**, *58*, 380–388.
- [53] I. Weissbuch, L. J. W. Shimon, E. M. Landau, R. Popovitzbiro, Z. Berkovitchyellin, L. Addadi, M. Lahav, L. Leiserowitz, *Pure Appl. Chem.* **1986**, *58*, 947–954.

Received: November 25, 2009

Revised: June 4, 2010

Published online: September 20, 2010